Differential Thermal Analysis and PVT Measurements on 2,2,2-Trichloro-ethanol Under High Pressure

M. Jenau, M. Sandmann, A. Würflinger, and J. Ll. Tamarit[a]

Institute of Physical Chemistry II, Ruhr-University, D-44780 Bochum, Germany
[a] Department de Física i Enginyeria Nuclear, Universitat Politècnica de Catalunya, Diagonal 647; 08028 Barcelona, Catalonia, Spain

Z. Naturforsch. **52a**, 493–501 (1997); received April 26, 1997

The phase behaviour, the calorimetric and volumetric properties of 2,2,2-trichloro-ethanol (TCE) have been studied with differential thermal analysis (DTA) and pVT measurements in the pressure range 1 atm to 300 MPa and temperatures between 250 K to 355 K. TCE displays a metastable plastic phase (solid I′) and a non-plastic solid phase II at atmospheric pressure. At least two pressure-induced solid phases have been detected: a stable plastic phase (solid I) and a non-plastic phase (solid III). There are two sets of triple points: a) 123 MPa and 308 K with the phases solid I, solid II and the liquid, b) 243 MPa and 316 K for solid I, II, III. Furthermore a metastable low-temperature brittle form (solid II′) has been found, which transforms to solid I at a considerably lower temperature than solid II. The melting curve of solid I′ can be pursued to higher pressures up to 260 MPa. On the other hand, the melting curve of the stable plastic phase solid I can be extrapolated beyond the triple point to pressures below 123 MPa. Volume and enthalpy changes are reported for all phase transitions.

1. Introduction

Recently we investigated the phase behaviour of a series of tertiary butyl compounds, which exhibit a rich polymorphism [1]. The molecular shape of 2,2,2-trichloro-ethanol (TCE) is related to 2,2-dimethyl-propanol (neopentanol) when replacing the methyl groups by chlorine atoms. Therefore TCE belongs to the classification of globular molecules, for which a rotator phase can be expected [2]. So far nothing is reported in literature about the phase behaviour of TCE at normal pressure, let alone at high pressures. It is the aim of the present work to establish the phase diagram and to determine the calorimetric properties and specific volumes for the liquid and solid phases.

2. Experimental

2.1 Differential Thermal Analysis

The transition temperatures are detected with the aid of a high pressure differential thermal analysis (DTA) apparatus in a pressure range up to 300 MPa. The previously described high pressure device [1, 3] is based on a design developed in the group of Schneider [4]. The transition temperatures were usually determined on heating runs at rates of about 1 K min^{-1}. The sample is filled in indium cells, which are then closed in order to avoid the solution of the pressure-transmitting gases (argon or helium). A heating and cooling system around the pressure vessel allows to apply specific annealing conditions. The calorimetric studies were supplemented by differential scanning calorimetry (DSC 7 Perkin Elmer) at atmospheric pressure in Barcelona.

Reprint requests to Prof. A. Würflinger;
Fax: +49 234 70 94 183.

2.2 PVT-Measurements

Specific volume data were obtained with the use of a recently improved high pressure dilatometer up to 300 MPa [5–7]. The sample is filled in a cylindrical steel cell closed by a moving piston, whose displacement is recorded inductively. The recorded volume changes along an isotherm are connected with the specific volumes at atmospheric pressure. Thus PVT data are established in the whole p, T range. The densities at normal pressure were determined with a commercial vibrating-tube densimeter Anton Paar DMA58. For further experimental details see [5–7].

2.3 Material

Commercially available 2,2,2-trichloroethanol (Aldrich, Germany) was dried over molecular sieve 4 Å. The purity of 99.5% was determined by gas chro-

0932-0784 / 97 / 0600-0493 $ 06.00 © – Verlag der Zeitschrift für Naturforschung, D-72027 Tübingen

matography. The samples were always manipulated in a glove box under dry argon gas.

3. General Phase Behaviour

3.1 Phase Behaviour at Atmospheric Pressure

When the sample is cooled in a DTA run from temperature it freezes at 270 K and melts at 273 K on reheating with low entropy of fusion. The small entropy change is obviously evidence that a plastic phase has been reached (denoted as solid I'). Therefore a further transition is expected at lower temperatures. In fact, below 258 K a new solid phase is obtained (see Fig. 1), which will be denoted SII in the following. However, reheating does not lead to a transition to the plastic phase but to melting at 292 K. The significantly higher melting temperature of solid II, as well as several runs with different annealing conditions prove that the plastic phase at atmospheric pressure is metastable. The DTA investigation was extended to lower temperatures of ~130 K, without any indication of further phase transitions. The heats of transition have been determined with DSC and are summarized in Table 1. The transition temperatures differ somewhat from the DTA results. The Table contains also enthalpy changes derived from ΔV measurements (see below).

Table 1. Thermodynamic Properties of TCE at 1 atm.

Transition	T/K (DSC)	ΔH kJ mol^{-1} (DSC)	ΔH kJ mol^{-1} (ΔV meas.)
Liquid → solid I'	269.4±1.1	0.89±0.11	
Solid I' → liquid	271.6±1.0	0.91±0.11	0.91
Solid I' → solid II	~260	6.98±0.30	
Solid II → liquid	290.6±1.0	10.05±0.42	10.78

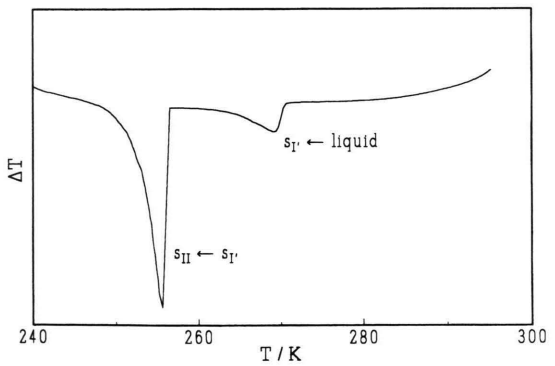

Fig. 1. DTA traces obtained on cooling at 1 atm, showing the freezing to solid I' and the solid I' → solid II transition.

3.2 Phase Behaviour at Higher Pressures

The phase diagram of TCE was established in the temperature range from 250 K to 355 K and pressures up to 300 MPa. Various pressure-induced stable and metastable phases have been detected, which render the phase situation very intricate. Starting with DTA, we found two new high-pressure phases (plastic solid I, and non-plastic solid III), and correspondingly two sets of triple points. In some DTA runs there was evidence of a further metastable non-plastic phase, denoted as solid II', which was corroborated by pVT measurements. In pVT measurements the pressure is usually changed along isotherms. Thus the approach to phase transitions is different from that in DTA, which may reveal quite new features. We present the phase behaviour in two figures 2a, b, because the phase boundaries of the many stable and metastable phases partly overlap in a confusing manner. Open symbols refer to DTA, full symbols to pVT measurements. The phase transitions between stable phases observed on heating are presented by solid lines. Phase transitions from metastable phases are plotted by dashed lines, those obtained on cooling by dotted lines.

3.2.1 High Pressure Phases I, I', and II

The transitions between the phases I, I', II, and the liquid are displayed in Figure 2a. In the low pressure region we observe the same phases (solid I' and II) as at atmospheric pressure. The metastable liquid phase between the two melting curves (II → liquid, I' → liquid) does not freeze to solid II, even after annealing of several days. Also the metastable plastic phase I' can be maintained for several hours. It does not convert spontaneously into solid II when the temperature is above the I' → II transition line.

The two melting curves converge with rising pressure and seem to intersect at about 150 MPa. However, above 130 MPa new phases appear. Nevertheless the freezing and the melting curves of solid I' can be continued to 260 MPa. Cooling the phase solid I' at higher pressures, however, does not yield solid II, but a second plastic phase solid I. Reheating of solid I gives a considerably higher melting temperature

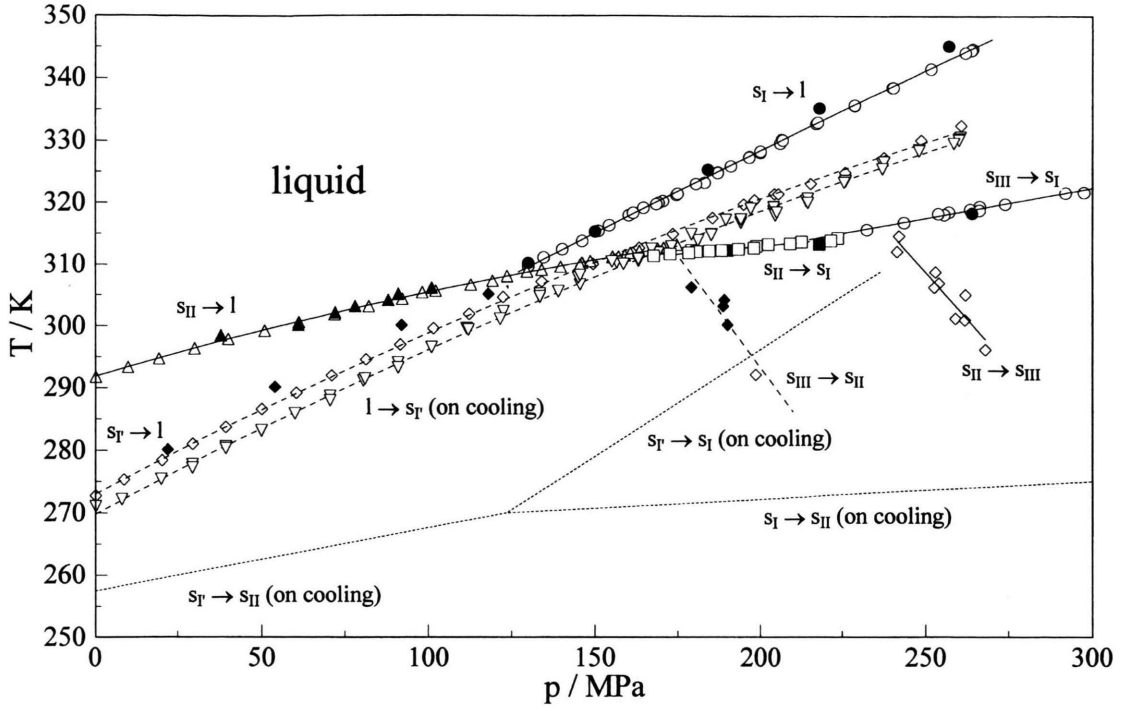

Fig. 2. a) Phase diagram of TCE, showing the solid phases I, I′, II, and III.

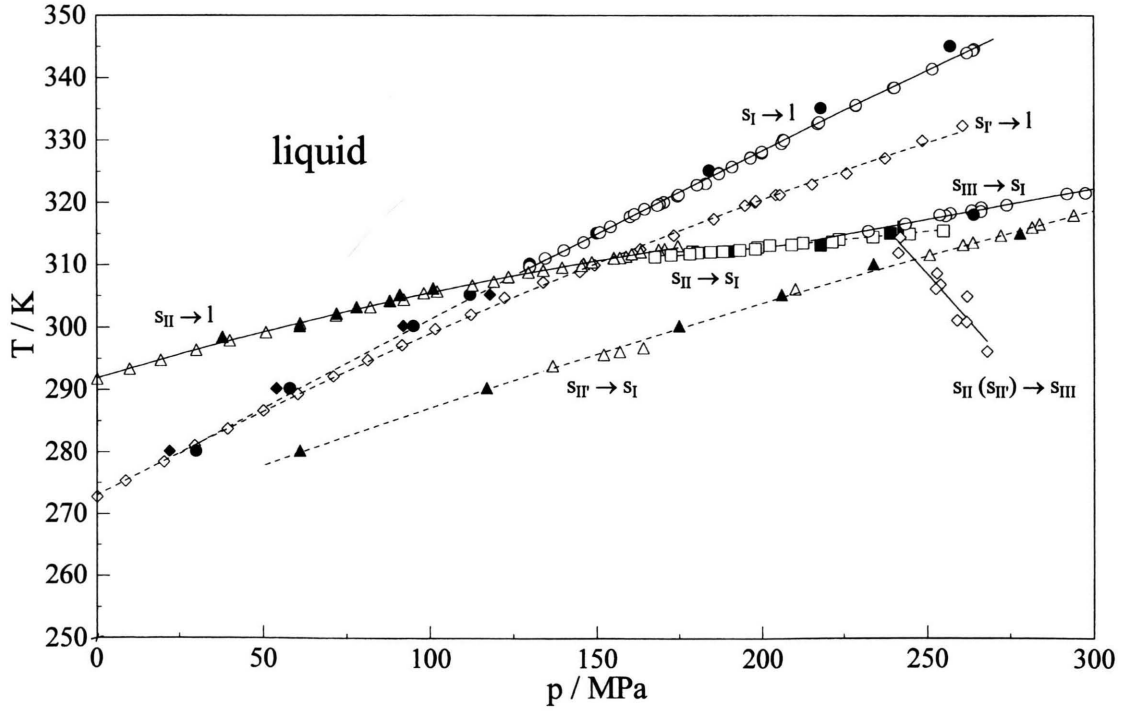

Fig. 2. b) Phase diagram of TCE, showing the metastable phase II′ and the extrapolated melting curve for solid I.

than SI′ → liquid. On further cooling of solid I it transforms into the non-plastic solid phase II, accompanied by a large enthalpy effect. A typical DTA run is displayed in Fig. 3a, showing the transitions liquid → I′ → I → II. On reheating solid II we obtain again solid phase I, so the transformation between I and II is enantiotropic, see Figure 3b. The phases solid I, solid II and the liquid meet at a triple point of 123 MPa and 308 K.

The phase behaviour, however, is more complicated. When the pressure in the experiment of Fig. 3 is reduced, the transitions II → I and I → liquid converge and cannot be separated below 167 MPa. Solid II then immediately melts, corresponding to the melting curve, which can be extrapolated from the low pressure region ($p < 123$ MPa). The extrapolated melting curve of solid II (to pressures > 123 MPa) practically coincides with the solid II → I phase boundary. Surprisingly, also the melting curve of solid I can be pursued beyond the triple point to lower pressures < 123 MPa, as was detected in pVT measurements (cf. Chapter 3.2.3). In this low pressure range, solid I is the second metastable plastic phase, not to be confused with solid S I′. Solid I is only observed in the low-pressure region, when solid II′ (see Chapter 3.2.3) has been generated in the high-pressure region. The extrapolated melting curve SI → liquid has been omitted in Fig. 2a, but is shown in Figure 2b.

The melting of solid I′ was also observed in the pressure-volume measurements on decreasing pressure along an isotherm, see Figure 4. The volume step is not very sharp, due to a pretransitional effect. Nevertheless, the extrapolated ΔH value (derived from the volume change with the aid of the Clausius-Clapeyron equation) agrees excellently with the result from DSC measurements, see Table 1. For this calculation the pretransitional effect was not incorporated in the volume change.

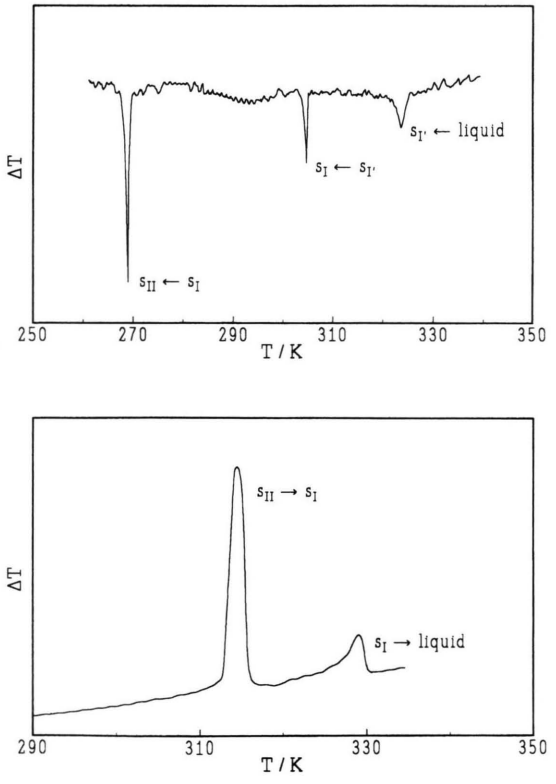

Fig. 3. a) DTA traces obtained on cooling about 230 MPa, showing the sequence liquid → I′ → I → II.

Fig. 3. b) DTA traces obtained on reheating, showing the transitions II → I → liquid.

3.2.2 High Pressure Phase Solid III

Above 240 MPa another pecularity is encountered. The transformation from low temperatures to phase I is preceded by an additional peak that is attributed to the transformation from solid II to a new phase solid III. In Fig. 5 we present DTA traces obtained at about 255 MPa. The DTA traces of Fig. 5a are assigned to the sequence II → III → I. In Fig. 5b two low-temperature transitions are observed with a much smaller peak area than in Figure 5a. It is assumed that this was caused by a mixture of two low-temperature brittle phases II and II′ (cf. next chapter). The transformation solid III → II could not be observed on cooling. However, a somewhat shifted transition (attributed to solid III → II) was detected on decreasing pressure along an isotherm. The triple point solid I, II, III is estimated to be located at 243 MPa and 316 K.

The transitions solid III → II, solid III → I, solid II → I, solid II → liquid, and solid I → liquid are clearly discovered in the pressure-volume measurements, see Figure 6. It can be immediately deduced from the isotherms that solid III is denser than solid II. Therefore it is understandable that solid III does not want to transform to solid II on cooling, however, decreasing pressure favours a transformation to a less dense phase. The volume change for the solid I → liquid is twice as large as that of the melting of solid I′.

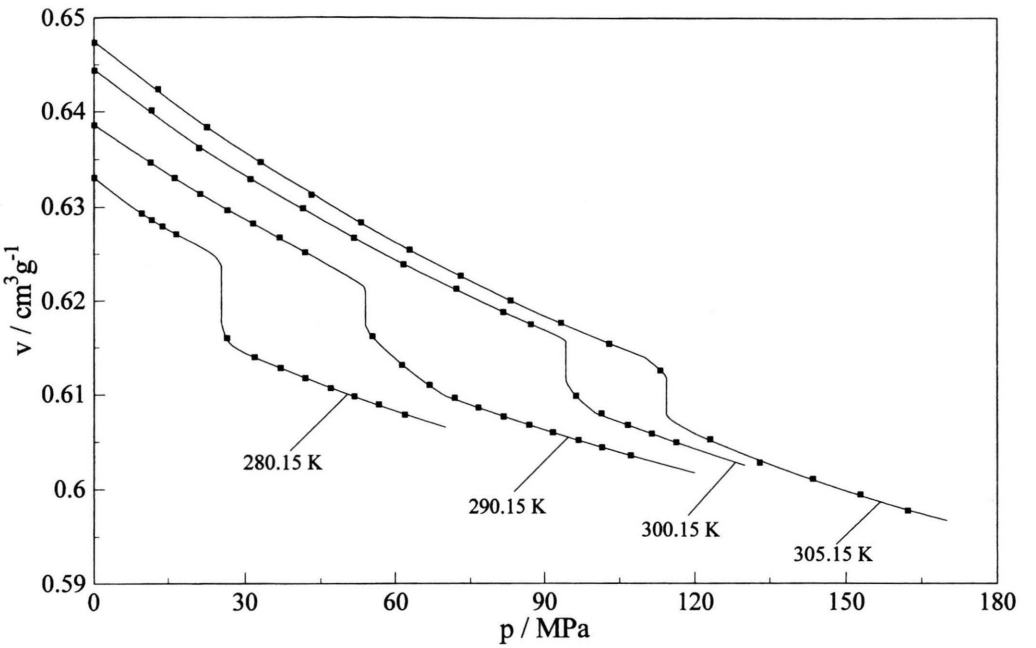

Fig. 4. Specific volumes as a function of pressure, in the neighbourhood of the melting of solid I'. TCE – $s_{I'} \rightarrow 1$.

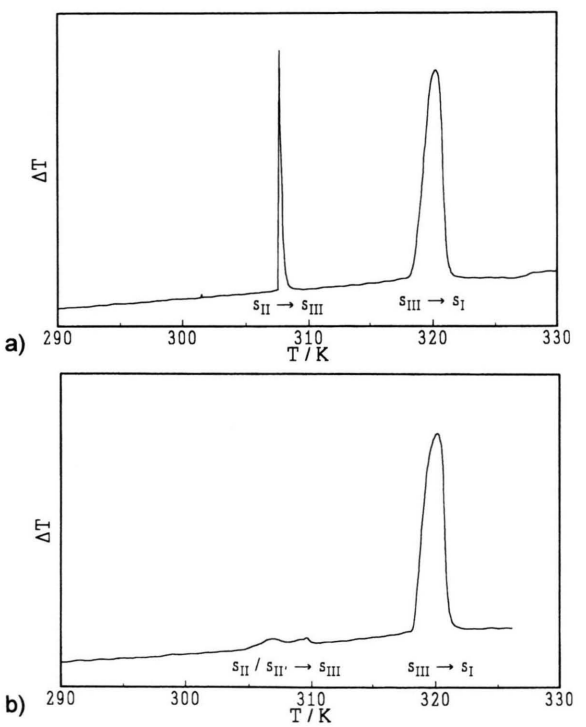

Fig. 5. a) DTA traces obtained about 255 MPa, showing the sequence solid II → III → solid I.

Fig. 5. b) DTA traces showing the transitions solid II (II') → III → I.

3.2.3 High-Pressure Phase Solid II'

In some DTA runs the transition to solid I was considerably shifted to lower temperatures. This transition is caused by the generation of a metastable phase solid II', as has been proved in extended DTA and pVT measurements. In the latter experiments solid II' was generated by pressurizing to 250–300 MPa at room temperature and then releasing the pressure step by step at constant temperature. Repeating this procedure at various temperatures yields the solid II' → I transition line displayed in Figure 2b. In Fig. 7 the specific volume is plotted as a function of pressure, showing the volume changes for the transitions solid II' → solid I and solid I → liquid. The lowest isotherm (280 K), however, displays a negative step, apparently due to the solid I → solid II transition on decreasing pressure. Note that below the triple point pressure (123 MPa) solid I is metastable (cf. Chapter 3.2.1). The low-temperature metastable phase solid II' was observed almost in the whole pressure range (50–300 MPa).

Repeated DTA experiments in the high pressure range yielded also transition points solid II' → solid I in the coexistence range of solid III. Thie means that the transition from solid II' → solid III (cf. Fig. 5b) has

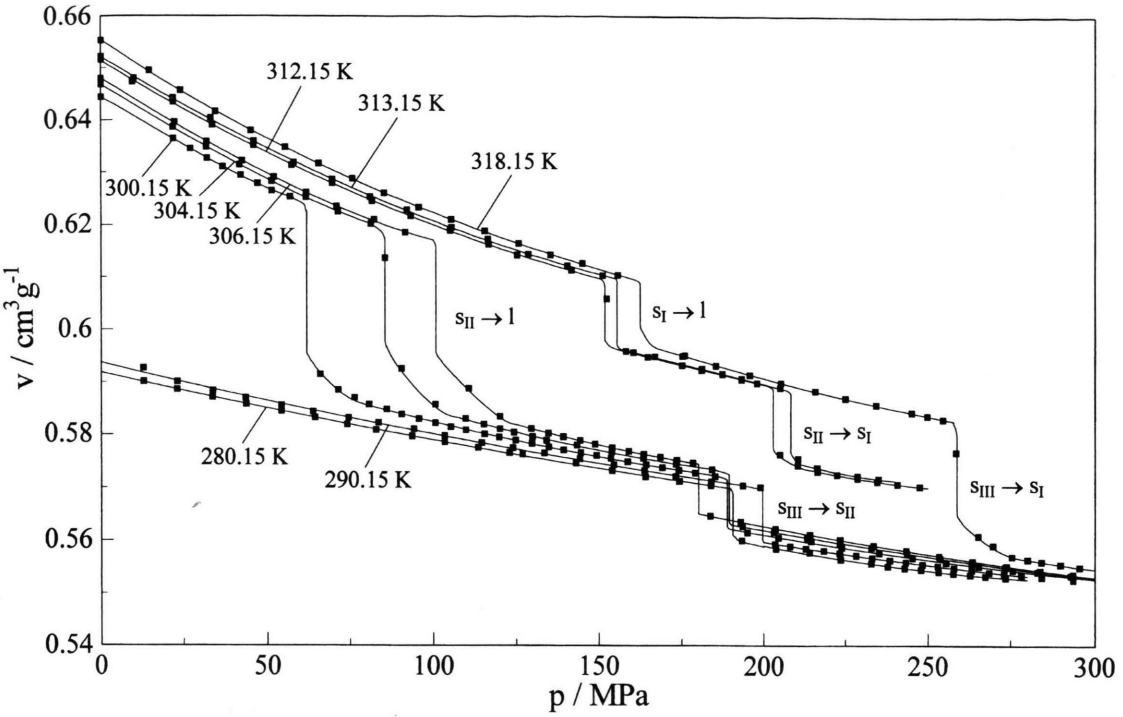

Fig. 6. Specific volumes as a function of pressure, the steps in the isotherms refer to the transitions: solid III → solid II, solid III → solid I, solid II → solid I, solid II → liquid, and solid I → liquid.

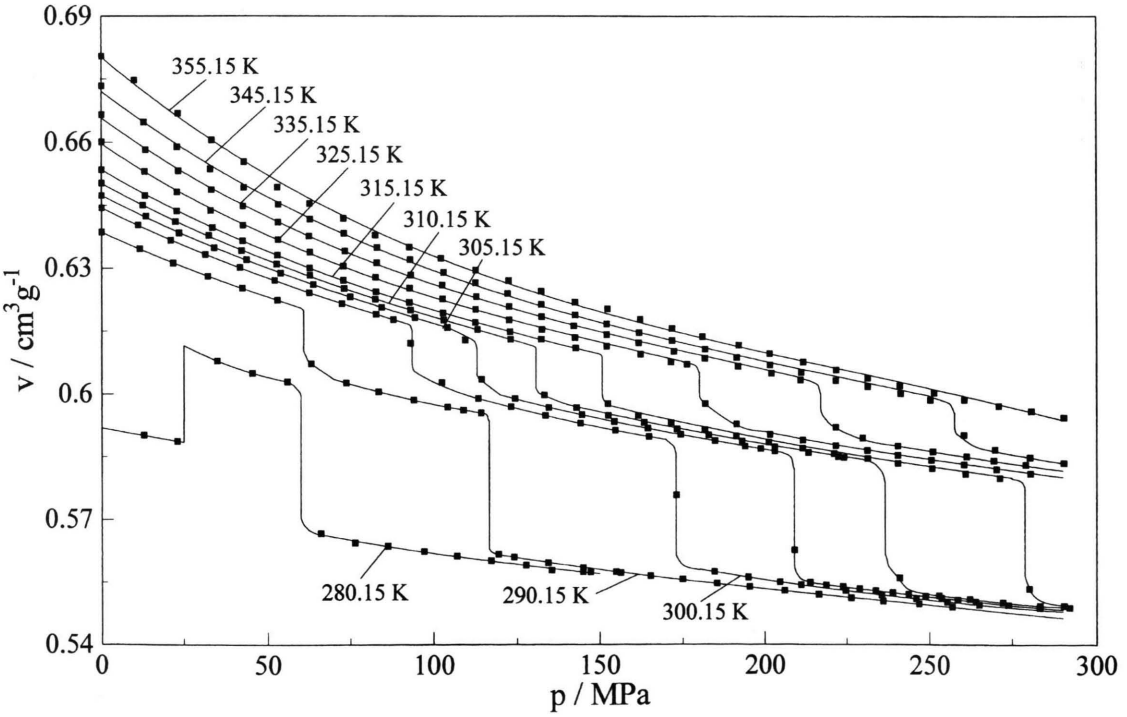

Fig. 7. Specific volumes as a function of pressure, the steps in the isotherms refer to the solid II′ → solid I transition and melting of solid I. TCE – $s_{II'} \rightarrow s_I \rightarrow l$.

been avoided. It seems that transitions connected with phase III are kinetically hindered.

4. Thermodynamic Properties and Phase Boundaries

The pressure dependences of the transition temperatures were fitted to polynomial functions:

$$T/\mathrm{K} = a + b \cdot p/\mathrm{MPa} + c \cdot (p/\mathrm{MPa})^2 ,$$

and are compiled in Table 2. Results from both DTA and pVT measurements have been incorporated in the fitting.

Volume and enthalpy changes (calculated with the use of the Clausius-Clapeyron equation) have been smoothed and are listed in Table 3. The largest volume changes are found for the transitions from the non-plastic phases S II → liquid and S II′ → S I. The smallest volume changes are observed for the melting of the disordered phases S I and S I′. The metastable phase solid II′ is much denser than the stable phase solid II.

The volume change of the phase transitions decreases with increasing pressure, that is a common finding in pVT measurements [1, 8–10]. The enthalpy change of the solid II′ → solid I transition increases somewhat with increasing pressure. Similar effects have been observed for the solid III → solid I transition of cyclohexane [8], the solid III → solid I transition of neohexanol [9], and the rotational transition of *n*-alkanes [10]. For most molecular crystals a decrease of ΔH with increasing pressure is observed [4].

The specific volume data are collected in the Tables 4 a, b, c (see page 500 and 501). A dash in the columns indicates a phase transition.

Table 2. Transition Temperatures as a Function of Pressure.

Transition	*a*	*b*	10^4 *c*
S I → liquid	272.41	0.296	−0.842
S I′ → liquid	273.33	0.284	−2.38
S II → liquid	291.89	0.157	−2.12
S II → S I	302.20	0.0533	
S II′ → S I	268.34	0.195	−0.888
S III → S I	292.94	0.0977	
S II → S III	458.76	−0.60	
S III → S II	436.17	−0.72	

Table 3. Thermodynamic Properties of TCE.

Phase transition	*T* K	*p* MPa	ΔV_m $cm^3 \cdot mol^{-1}$	ΔH_m $kJ \cdot mol^{-1}$	ΔS_m $J \cdot K^{-1} \cdot mol^{-1}$
S I′ → liquid	272.75	0.1	0.95	0.91	3.34
	280.15	22	0.91	0.92	3.33
	290.15	54	0.84	0.94	3.26
	300.15	92	0.77	0.96	3.21
	305.15	118	0.72	0.96	3.16
S II → liquid	291.75	0.1	5.90	10.78	36.97
	300.15	61	4.60	10.53	35.07
	302.15	72	4.37	10.44	34.54
	304.15	88	4.03	10.24	31.15
	306.15	101	3.75	10.05	30.77
S I → liquid	280.15	25			
	290.15	58	2.07	2.10	7.22
	300.15	95	1.99	2.13	7.10
	305.15	112	1.95	2.14	7.03
	310.15	130	1.91	2.16	6.96
	315.15	150	1.86	2.16	6.86
	325.15	184	1.78	2.18	6.71
	335.15	218	1.70	2.19	6.55
	345.15	257	1.61	2.20	6.31
S II → S I	312.15	199	2.26	13.24	42.40
	313.15	211	2.16	12.69	40.53
S II′ → S I	280.15	61	5.17	7.86	28.07
	290.15	117	4.97	8.28	28.53
	300.15	175	4.77	8.73	29.10
	305.15	206	4.66	8.98	29.41
	310.15	234	4.56	9.22	29.72
	315.15	278	4.41	9.54	30.28
S III → S I	318.15	264	2.64	8.60	27.02
S III → S II	280.15	189	1.45	−0.57	−2.03
	290.15	201	1.53	−0.62	−2.14
	300.15	190	1.49	−0.63	−2.08
	304.15	189	1.48	−0.63	−2.07
	306.15	181	1.40	−0.60	−1.96

5. Concluding Remarks

TCE displays a rich polymorphism that is quite unexpected. The finding of stable and metastable plastic phases in the high pressure range resembles the dual melting curves of carbon tetrachloride [11] at ambient pressure. In the low-pressure range of TCE, however, three different melting curves are observed that have not been described before. Low-temperature metastable phases and monotropic transitions have often been found in plastic and liquid crystals [12]. We have shown in this work that DTA and pVT measurements are complementary experimental methods, which give useful insight in the phase behaviours of molecular crystals.

Table 4a. Specific volumes ($g^{-1} \cdot cm^3$) of TCE for the phases liquid, I, and II′.

p/MPa	T/K									
	280.15	290.15	300.15	305.15	310.15	315.15	325.15	335.15	345.15	355.15
0.1	0.592	0.639	0.644	0.647	0.650	0.654	0.660	0.666	0.672	0.680
10	0.590	0.635	0.641	0.643	0.646	0.649	0.655	0.660	0.666	0.674
20	0.589	0.632	0.637	0.640	0.642	0.645	0.650	0.655	0.661	0.668
30	0.609	0.629	0.634	0.637	0.639	0.641	0.646	0.651	0.656	0.662
40	0.606	0.626	0.631	0.633	0.635	0.637	0.642	0.646	0.651	0.657
50	0.604	0.623	0.628	0.630	0.632	0.634	0.638	0.642	0.647	0.652
60	0.602	0.606	0.625	0.627	0.629	0.631	0.634	0.639	0.643	0.648
70	0.566	0.603	0.622	0.624	0.624	0.628	0.631	0.635	0.639	0.644
80	0.564	0.601	0.620	0.621	0.623	0.625	0.628	0.632	0.636	0.640
90	0.563	0.599	0.617	0.619	0.621	0.623	0.626	0.629	0.633	0.636
100	0.562	0.597	0.602	0.616	0.618	0.620	0.623	0.626	0.629	0.633
110	0.561	0.596	0.599	0.614	0.616	0.618	0.621	0.624	0.627	0.630
120	0.560	0.561	0.597	0.600	0.614	0.616	0.618	0.621	0.624	0.627
130	0.559	0.560	0.595	0.598	0.612	0.614	0.616	0.619	0.622	0.624
140	0.558	0.559	0.594	0.596	0.598	0.612	0.614	0.617	0.619	0.622
150	0.557	0.558	0.592	0.594	0.596	0.610	0.612	0.615	0.617	0.620
160		0.557	0.590	0.592	0.594	0.596	0.611	0.613	0.615	0.618
170		0.556	0.589	0.591	0.592	0.594	0.609	0.611	0.613	0.616
180		0.555	0.558	0.589	0.591	0.592	0.607	0.609	0.611	0.614
190		0.554	0.557	0.588	0.590	0.591	0.593	0.608	0.610	0.612
200		0.553	0.556	0.587	0.588	0.589	0.591	0.606	0.608	0.610
210		0.553	0.554	0.555	0.587	0.588	0.590	0.604	0.606	0.608
220		0.552	0.553	0.554	0.586	0.586	0.588	0.591	0.605	0.607
230		0.551	0.552	0.553	0.584	0.585	0.587	0.589	0.603	0.605
240		0.550	0.551	0.552	0.553	0.584	0.586	0.588	0.601	0.603
250		0.549	0.550	0.551	0.552	0.583	0.584	0.586	0.600	0.601
260		0.549	0.550	0.551	0.551	0.581	0.583	0.585	0.588	0.600
270		0.548	0.549	0.550	0.550	0.580	0.582	0.584	0.586	0.598
280		0.547	0.549	0.549	0.550		0.581	0.583	0.585	0.596
290		0.546	0.548	0.548	0.549		0.580	0.581	0.583	0.594

Acknowledgements

One of us (J. Ll. T.) acknowledges the financial support of the DGICYT (grant PB95-0032). We thank also Fonds der Chemie for financial support.

[1] J. Reuter, D. Büsing, J. Ll. Tamarit, and A. Würflinger, J. Mater. Chem. **7,** 41 (1997); M. Jenau, J. Reuter, J. Ll. Tamarit, and A. Würflinger, J. Chem. Soc. Faraday Trans. **92,** 1899 (1996).

[2] J. Timmermans, Bull. Soc. Chim. Belges **44,** 17 (1935); J. Chim. Physique **35,** 331 (1938); J. Phys. Chem. Solids **18,** 1 (1961).

[3] A. Würflinger, Ber. Bunsenges. Phys. Chem. **79,** 1195 (1975); N. Pingel, U. Poser, and A. Würflinger, J. Chem. Soc. Faraday Trans I, **80,** 3221 (1984).

[4] C. Schmidt, M. Rittmeier-Kettner, H. Becker, J. Ellert, R. Krombach, and G. M. Schneider, Thermochim. Acta **238,** 321 (1994); M. Kuballa, and G. M. Schneider, Ber. Bunsenges. Phys. Chem. **75,** 513 (1971).

[5] R. Landau and A. Würflinger, Rev. Sci. Instrum. **51,** 533 (1980).

[6] M. Jenau, doctoral thesis, Ruhr-Universität Bochum (1996). Note that in the thesis solid III was denoted as solid II″.

[7] M. Sandmann, doctoral thesis, Ruhr-Universität Bochum, in preparation.

[8] K. D. Wisotzki and A. Würflinger, J. Phys. Chem. Solids **43,** 13 (1982).

[9] R. Edelmann, U. Bardelmeier, and A. Würflinger, J. Chem. Soc. Faraday Trans. **87,** 1149 (1991); R. Edelmann, and A. Würflinger, Mol. Cryst. Liq. Cryst. **195,** 281 (1991).

[10] R. Landau and A. Würflinger, Ber. Bunsenges. Phys. Chem. **84,** 895 (1980); R. R. Nelson, W. Webb, and J. A. Dixon, J. Chem. Phys. **33,** 1756 (1960); M. Kamphausen and G. M. Schneider, Thermochim. Acta **22,** 371 (1978).

[11] U. Bardelmeier and A. Würflinger, Thermochim. Acta **143,** 109 (1989).

[12] M. Hartmann, M. Jenau, A. Würflinger, M. Godlewska, and S. Urban, Z. Physik. Chem. Frankfurt **177,** 195 (1992); A. Würflinger, Int. Rev. Phys. Chem. **12,** 89 (1993).

Table 4b. Specific volumes ($g^{-1} \cdot cm^3$) of TCE for the phases liquid, I'.

p/MPa	T/K			
	280.15	290.15	300.15	305.15
0.1	0.633	0.639	0.644	0.648
5	0.631	0.637	0.642	0.645
10	0.629	0.635	0.641	0.643
15	0.628	0.633	0.639	0.641
20	0.626	0.632	0.637	0.639
25	0.616	0.630	0.635	0.638
30	0.614	0.629	0.633	0.636
35	0.613	0.627	0.632	0.634
40	0.612	0.626	0.630	0.632
45	0.611	0.624	0.628	0.631
50	0.610	0.623	0.627	0.629
55	0.609	0.613	0.625	0.628
60	0.608	0.612	0.624	0.626
65	0.607	0.611	0.623	0.625
70	0.607	0.610	0.622	0.623
75		0.609	0.620	0.622
80		0.608	0.619	0.621
85		0.607	0.618	0.620
90		0.606	0.617	0.618
95		0.605	0.609	0.617
100		0.605	0.608	0.616
110		0.603	0.606	0.614
120			0.604	0.606
130				0.604
140				0.602
150				0.600
160				0.598
170				0.597

Table 4c. Specific volumes ($g^{-1} \cdot cm^3$) of TCE for the phases S II, S III (280.15 K – 290.15 K), liquid, S II, S III (300.15 K – 306.15 K), liquid, S I, S II (312.15 K – 313.15 K), and liquid, S I, S III (318.15 K).

p/MPa	T/K							
	280.15	290.15	300.15	304.15	306.15	312.15	313.15	318.15
0.1	0.592	0.594	0.644	0.647	0.648	0.652	0.652	0.655
10	0.591	0.592	0.641	0.643	0.644	0.648	0.648	0.651
20	0.589	0.591	0.637	0.639	0.640	0.644	0.645	0.647
30	0.588	0.589	0.634	0.636	0.637	0.641	0.641	0.644
40	0.586	0.588	0.630	0.632	0.633	0.637	0.638	0.640
50	0.585	0.587	0.627	0.629	0.630	0.634	0.635	0.637
60	0.584	0.585	0.624	0.626	0.627	0.631	0.632	0.634
70	0.583	0.584	0.587	0.623	0.624	0.628	0.629	0.631
80	0.581	0.583	0.585	0.621	0.621	0.625	0.626	0.628
90	0.580	0.581	0.584	0.590	0.619	0.623	0.623	0.625
100	0.579	0.580	0.582	0.586	0.617	0.620	0.621	0.622
110	0.578	0.579	0.581	0.583	0.586	0.618	0.619	0.620
120	0.577	0.578	0.580	0.581	0.584	0.616	0.616	0.618
130	0.576	0.577	0.578	0.580	0.581	0.614	0.614	0.616
140	0.575	0.576	0.577	0.578	0.580	0.612	0.612	0.614
150	0.574	0.575	0.576	0.577	0.578	0.597	0.598	0.612
155	0.573	0.574	0.575	0.577	0.577	0.596	0.597	0.611
160	0.573	0.574	0.575	0.576	0.577	0.596	0.596	0.610
165	0.572	0.573	0.574	0.575	0.576	0.595	0.595	0.598
170	0.572	0.573	0.574	0.575	0.576	0.594	0.594	0.597
175	0.571	0.572	0.573	0.574	0.575	0.593	0.594	0.595
180	0.571	0.572	0.573	0.574	0.575	0.593	0.593	0.594
185	0.570	0.571	0.572	0.573	0.565	0.592	0.592	0.593
190	0.560	0.571	0.562	0.563	0.564	0.591	0.591	0.592
195	0.560	0.570	0.562	0.563	0.563	0.590	0.590	0.592
200	0.559	0.570	0.561	0.562	0.563	0.590	0.590	0.591
205	0.558	0.559	0.561	0.561	0.562	0.575	0.589	0.590
210	0.558	0.559	0.560	0.561	0.562	0.574	0.575	0.589
215	0.557	0.558	0.560	0.560	0.561	0.573	0.574	0.588
220	0.557	0.558	0.559	0.560	0.560	0.573	0.573	0.588
225	0.556	0.557	0.559	0.559	0.560	0.572	0.573	0.587
230	0.556	0.557	0.558	0.559	0.559	0.572	0.572	0.586
235	0.555	0.557	0.558	0.558	0.559	0.571	0.572	0.586
240	0.555	0.556	0.557	0.558	0.558	0.571	0.571	0.585
245	0.555	0.556	0.557	0.557	0.558			0.584
250	0.554	0.555	0.556	0.557	0.557			0.584
255	0.554	0.555	0.556	0.556	0.557			0.583
260	0.553	0.555	0.556	0.556	0.556			0.582
265	0.553	0.554	0.555	0.556	0.556			0.560
270	0.553	0.554	0.555	0.555	0.556			0.558
275			0.554	0.555	0.555			0.557
280			0.554	0.554	0.555			0.556
285			0.554	0.554	0.554			0.556
290			0.553	0.553	0.554			0.555